A Theoretical Study of the Essential Role of DMSO as a Solvent/Ligand in the $Pd(OAc)_2$/DMSO Catalyst System for Aerobic Oxidation

Wiktor Zierkiewicz† and Timofei Privalov*

Department of Chemistry, Royal Institute of Technology (KTH), S-10044 Stockholm, Sweden

Received July 25, 2005

Dimethyl sulfoxide (DMSO) has unique properties as an aprotic, polar solvent. The oxygen atom in DMSO can interact with positive charges and thus stabilize metal cation. The sulfur atom, although somewhat positively charged, does not interact with negative charges effectively. Also, two methyl groups surround the sulfur atom and influence binding properties of DMSO. These features of DMSO are addressed in the present computational study of the $Pd(AcO)_2$/DMSO-catalyzed aerobic oxidation system. Mechanistic and computational details are provided. The step-by-step Gibbs energy of reaction was calculated using the electronic energy at the B3LYP density functional level with thermal functions calculated at the same level of theory. The solvent was modeled using the polarized medium (PCM) with additional DMSO molecules in the second coordination sphere of the complexes studied. The overall reaction pathway was divided into several steps in accord with available experimental data. All steps, including the first deprotonation and the β-hydride elimination transition states, were elucidated in good detail. Coordination and reorganization of DMSO in $Pd(II)(AcO)_2$/DMSO and $Pd(0)/(DMSO)_n$ complexes has been studied to provide realistic data about coordination of DMSO with hard (O) versus soft (S) ligand donor atoms. The β-hydride elimination transition state was identified computationally to give an estimation of the activation energy of the alcohol oxidation reaction. Therefore, we suggest that the rate-determining step is related to the alcohol part of the reaction cycle.

Introduction

During the past 10 years, many effective palladium catalyst systems have been developed for aerobic oxidation reactions.[1] Through mechanistic studies of Pd-catalyzed aerobic alcohol oxidations, a generally accepted mechanism has been developed in rather good detail (Scheme 1).[2]

In some recent studies,[3] we have investigated the overall mechanism of Pd-catalyzed aerobic oxidation in several systems with nonpolar solvent (toluene) and with the nitrogen-based ligands, i.e., pyridine and TEA.

Scheme 1. Mechanistic Outline of the Pd-Catalyzed Aerobic Alcohol Oxidation[a]

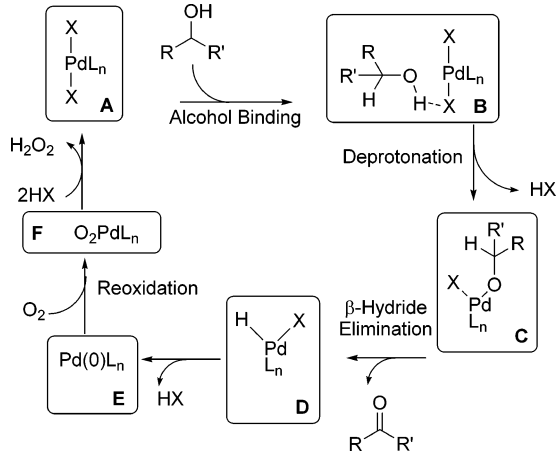

[a] X = AcO; L = DMSO.

The focus was on the alcohol-related parts of the oxidation reaction. The alcohol-related transition states and kinetic isotope effects were studied using experimental and quantum chemical methods. The latter require a reasonably good model of the reaction mechanism in order to justify comparison with experiment.

* Corresponding author. E-mail: priti@kth.se.
† On leave from Institute of Inorganic Chemistry, Wrocław University of Technology, Wybrzeze Wyspianskiego 27, 50-370 Wrocław, Poland.

(1) For up to date reviews and excellent references, see: (a) Sheldon, R. A.; Arends, I. W. C. E.; Dijksman, A. *Catal. Today* **2000**, *57*, 157−166. (b) Sheldon, R. A.; Arends, I. W. C. E.; ten Brink, G.-J.; Dijksman, A. *Acc. Chem. Res.* **2002**, *35*, 774−781. (c) Muzart, J. *Tetrahedron* **2003**, *59*, 5789−5816. (d) Stahl, S. S. *Angew. Chem., Int. Ed.* **2004**, *43*, 3400−3420. (e) Nishimura, T.; Ohe, K.; Uemura, S. *Synlett* **2004**, 201−216.

(2) For other mechanistic investigations on Pd-catalyzed aerobic alcohol oxidations, see: (a) Steinhoff, B. A.; Fix, S. R.; Stahl, S. S. *J. Am. Chem. Soc.* **2002**, *124*, 766−767. (b) Mueller, J. A.; Jensen, D. R.; Sigman, M. S. *J. Am. Chem. Soc.* **2002**, *124*, 8202−8203. (c) ten Brink, G.-J.; Arends, I. W. C. E.; Sheldon, R. A. *Adv. Synth. Catal.* **2002**, *344*, 355−369. (d) ten Brink, G.-J.; Arends, I. W. C. E.; Hoogenraad, M.; Verspui, G.; Sheldon, R. A. *Adv. Synth. Catal.* **2003**, *345*, 497−505. (e) Mueller, J. A.; Sigman, M. S. *J. Am. Chem. Soc.* **2003**, *125*, 7005−7013. (f) Trend, R. M.; Stoltz, B. M. *J. Am. Chem. Soc.* **2004**, *126*, 4482−4483. (g) Nielsen, R. J.; Keith, J. M.; Stoltz, B. M.; Goddard, W. A., III. *J. Am. Chem. Soc.* **2004**, *126*, 7967−7974. (h) Mueller, J. A.; Goller, C. P.; Sigman, M. S. *J. Am. Chem. Soc.* **2004**, *126*, 9724−9734. (i) Konnick, M. M.; Guzei, I. A.; Stahl, S. S. *J. Am. Chem. Soc.* **2004**, *126*, 10212−10213. (j) Steinhoff, B. A.; Guzei, I. A.; Stahl, S. S. *J. Am. Chem. Soc.* **2004**, *126*, 11268−11278.

(3) (a) Paavola, S.; Zetterberg, K.; Privalov, T.; Csöregh, I.; Moberg, C. *Adv. Synth. Catal.* **2004**, *346*, 237−244. (b) Privalov, T.; Linde, C.; Zetterberg, Z.; Moberg, C. *Organometallics* **2004**, *24*, 885−893. (c) Schultz, M.; Adler, R.; Zierkiewicz, W.; Privalov, T.; Sigman, M. *J. Am. Chem. Soc.* **2005**, *127*, 8499−8507.

10.1021/om0506217 CCC: $30.25
Publication on Web 10/19/2005

Scheme 2. Outline of the Reaction That Is Studied Computationally According to the Mechanism Presented in Scheme 1 in the Present Communication[a]

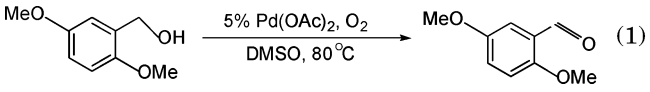

[a] Noteworthy, experimental results exclude mechanisms that involve DMSO redox chemistry.

However, solvent effects were small mainly because of low polarity of the solvent. The continuum solvent model (PCM) was totally sufficient and accurate in computing solvent correction to the reaction energy.

In the present study we will use the density functional method to describe the thermodynamics and the reaction mechanism of the more complex reaction 1 in polar dimethyl sulfoxide (DMSO) solvent (Scheme 2). The complexity stems from the rather unique coordination ability of DMSO: DMSO offers access to both hard (O) and soft (S) ligand donor atoms. This flexibility is expected to influence the reaction steps. In particular one may expect that it will facilitate the reoxidation from Pd(0) to Pd(II) in reaction 1 and similar reactions. DMSO is also a quite polar solvent. The dielectric constant of DMSO is lower than that of water but much higher than that of a typical pure hydrocarbon solvent. Solvating properties of DMSO allow stabilization of positive charges in solution, but DMSO does not provide an effective way to solvate and stabilize anions. The analysis of Pd(II)/DMSO and Pd(0)/DMSO complexes has implications well beyond the aerobic oxidation reaction with Pd-catalytic systems. To achieve the desired knowledge, a model with a considerably large amount of solvent molecules must be considered and compared with the traditional continuum approach.

Quantum chemistry methods seem to be well suited for studies of large Pd/DMSO complexes involved in an interaction with a solvent, while the aggregation/decomposition problem has proved to be difficult to study computationally. Thus, our main goal is to uncover the role of DMSO in the aerobic oxidation of alcohol, reaction 1, with means of computational chemistry and with the focus on metal-solvent/ligand complexes. All computations are performed according to the commonly adopted and well-tested strategy (see ref 3 and Technical Details section for more information).

Mechanistic Model of the Oxidation of an Alcohol and an Overview of the Reaction Profile. To initiate the computational study of reaction 1, an overview of the reaction profile and mechanistic model is necessary (Scheme 2).

The first part of the mechanism constitutes the oxidation of an alcohol with the change of oxidation state of the metal catalyst from Pd(II) to Pd(0). This part of the reaction has already been studied rather well for other types of palladium(II) catalysts. Dual coordinating ability of DMSO and relatively high dielectric constant both make the difference in the study we are going to undertake. Pd-pyridine or Pd-TEA systems, which we have previously studied, have the advantage and the simplification of a rather well-defined coordination geometry/structure of metal complexes by explicit definition of the ligand that coordinates to the metal. Furthermore, TEA and pyridine both have only one atom that coordinates to the metal. The distinction between ligand and solvent is somewhat less definite in the present study, and it relies on the proximity of a given DMSO molecule with respect to the metal. Those DMSO molecules that are bound in the first coordination sphere of Pd(II)/Pd(0) are ligands, while the rest of DMSO surrounding is solvent.

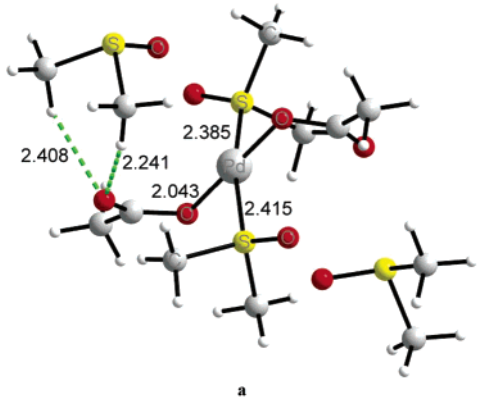

Figure 1. Optimized structure of monomeric Pd(II)$(AcO)_2$-$(DMSO\text{-}S)_2[DMSO]_2$ catalytic complex with two DMSO molecules in the first coordination sphere of palladium(II) and two DMSO in the outer parts of the complex. The projection of the picture is chosen to illuminate the interaction of DMSO with the O_{AcO} atom (dashed green lines). (Further in the text DMSO-S and DMSO-O always indicate the sulfur- and oxygen-bonded ligands, respectively.)

Pd(II)$(AcO)_2(DMSO)_2$ in Solvent Environment. Our starting point is DFT geometry optimization of the gas-phase monomeric Pd(II)$(AcO)_2(DMSO)_2[DMSO]_2$ "super molecule" (**a**, Figure 1). Both DMSO molecules are S-bound to palladium(II) as the result of unconstrained geometry optimization and in agreement with known crystal strucutres.[4,5] The role of additional DMSO molecules is to enhance the flexibility of the model with respect to intermolecular interactions. Intermolecular interactions via H-bonds are expected to be important for the crystal formation (see later, see also Supporting Information where computed and crystal structures are compared). DMSO in the second coordination sphere is important for stability of the complex **a**: additional DMSO interacts with the partially negatively charged oxygen atom of AcO^- (see Figure 1).[6] In the absence of these additional DMSO molecules the model becomes rather limited. One can see that O-bound DMSO is

(4) The ambidentate character of DMSO is quite remarkable. It has been demonstrated that the mode of DMSO coordination depends strongly on the interaction with the environment and by the effective electonegativity of the ligands coordinated to the metal center. See: Cotton, F. A.; Dikarev, E, V.; Petrukhina, M. A.; Striba, S.-E. *Inorg. Chem.* **2000**, *39*, 1748−1754, and references therein.

(5) In the crystal structure of $(DMSO)_2Pd(OAc)_2$ both DMSO ligands are S-bond and the complex is dimeric with only one DMSO ligand at each end. See: (a) Bancroft, D. P.; Cotton, F. A.; Verbruggen, M. *Acta Crystallogr. Sect. C* **1989**, *45*, 1289−1292. However, the palladium(II) trifluoroacetate crystal structure has one S-bound and one O-bound DMSO. See: (b) Stash, A. I.; Perepelkova, T. I.; Kravtsova, S. V.; Noskov, Yu. G.; Romm, I. P. *Russ. J. Coord. Chem.* **1998**, *24*, 36−39. (c) Tanaka, D.; Romeril, S. P.; Myers. A, G. *J. Am. Chem. Soc.* **2005**, *127*, 10323−10333. Interestingly, X-ray crystallographic characterization of arylpalladium(II) trifluroacetates shows two S-bound DMSO ligands. See ref 5c. Palladium(II) trifluoroacetate structure was computationally evaluated and found in very good agreement with the X-ray crystal structure reported in ref 5c.

(6) Interestingly, the preference of sulfur over oxygen in $(DMSO)_2Pd(OAc)_2$ is easy to verify directly within one geometry optimization sequence (see details in Supporting Information).

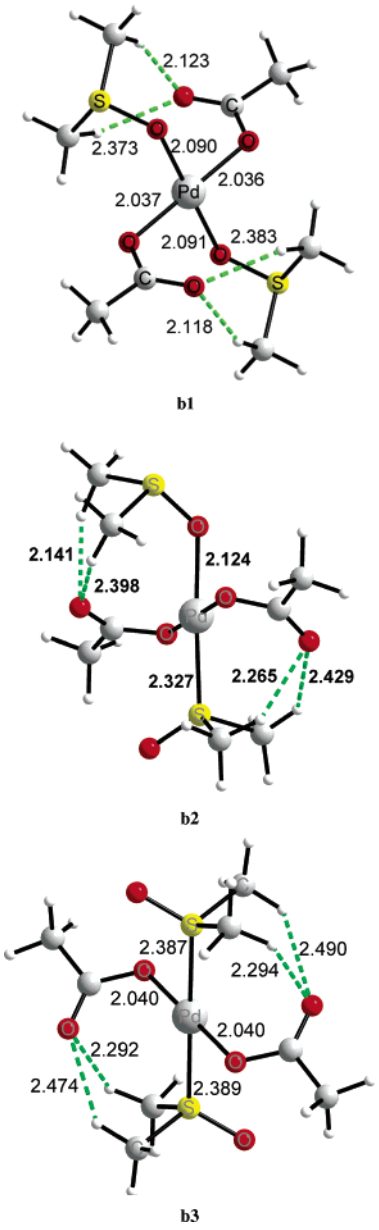

Figure 2. Optimized structure of the Pd(II)$(AcO)_2$ catalytic complex with only two DMSO molecules. **b1**: Pd(II)$(AcO)_2$ (DMSO-O)$_2$, S−O bond is 1.559 Å. **b2**: Pd(II)$(AcO)_2$ (DMSO-O)(DMSO-S), S−O bond is 1.554 Å for O-bound DMSO and S−O bond is 1.495 Å for S-bound DMSO. **b3**: Pd(II)$(AcO)_2$ (DMSO-S)$_2$, S−O bound is 1.496 Å. Dashed lines mark weak O−H bonding. All bond length parameters are in Å. S−O is 1.511 Å in free DMSO at the same level of theory.

better positioned to establish a weak intermolecular interaction than the S-bound ligand (see Figure 2).

To illuminate the importance of intermolecular interaction, we have considered only isolated Pd(II)$(AcO)_2$-(DMSO)$_2$. Judging by the final electronic energy in the gas phase, the O-bound Pd(II)/DMSO complex, **b1**, is the most stable. The second most stable one is the "mixed" S- and O-Pd(II)/DMSO complex, **b2**. The energy difference is about 2 kcal/mol. Finally the electronic energy of the purely S-bond Pd(II)/DMSO complex, **b3**, is larger than that of **b1** by almost 6 kcal/mol. The obvious discrepancy of these results with those obtained in the presence of two extra DMSO could be rationalized by intermolecular interactions. Indeed, one can observe

Table 1. Relative Energies of Pd$(AcO)_2$(DMSO)$_2$ Complexes with Different Coordination of DMSO Molecules[a]

	gas phase	single point in solvent	optimization in solvent
Pd$(AcO)_2$(DMSO-O)$_2$	0	0	0
Pd$(AcO)_2$(DMSO-O)(DMSO-S)	1.8	1.7	2.4
Pd$(AcO)_2$ (DMSO-S)$_2$	6	2.1	3.7

[a] Relative energies are obtained within three different approaches: (i) gas-phase geometry optimization without solvent effects; (ii) single-point calculation of the energy in solvent (PCM) at the gas-phase-optimized geometry; (iii) complete geometry optimization in solvent with PCM. All energies are in kcal/mol. The larger model, Pd(II)$(AcO)_2$(DMSO)$_2$[DMSO]$_2$, predicts S-bound DMSO, in agreement with the crystal structure.

a weaker intermolecular interaction due to the elongation of O_{AcO}−H_{DMSO} bonds in the case of S-bound DMSO. In the simple model, metal-bound DMSO interacts directly with AcO^-, while in the model with two extra DMSO a similar interaction occurs mainly between AcO^- and free DMSO.

The absolute value of the binding energy of one DMSO in the second coordination sphere is only about 4 to 7 kcal/mol. DMSO molecules in the extended model (see Figure 1) adjust their orientation and position in the second coordination sphere, and thus a more realistic description of S- or O-bonding to the metal can be achieved. A smaller model with just two DMSO molecules lacks this flexibility and favors O-bound DMSO because of a stronger intermolecular interaction.

The continuum model (PCM) provides a rather realistic description of polar solvent media, and thus weak intermolecular O_{AcO}−H_{DMSO} bonds become less important when dielectric screening is taken into account. Energies obtained by single-point calculations in the continuum solvent model demonstrate the decrease in the energy differences between **b1** and **b3** (see Table 1). (These "single-point solvent" calculations are performed on the basis of gas-phase-optimized geometry.)

A more accurate determination of relative energies in solvent may be obtained by geometry optimization with DFT methods including self-consistent optimization of solvent/reaction field at each geometry optimization step. Results agree well with simple single-point evaluation of the solvent energy (see Table 1). The energy difference of 2 or 3 kcal/mol is quite small, and it is important to realize that it is below the accuracy of the density functional method itself. Therefore it is quite arbitrary to differentiate between complexes **b1** and **b2** at the present level of theory within a simple two-DMSO model. The relative energy of **b1** and **b3** is somewhat larger but still small compared to the 5 kcal/mol accuracy of the method itself.

Comparison of gas-phase and solvent results points out a large influence of dielectric screening on the relative energy even in the most simple cases of isolated Pd$(AcO)_2$/DMSO complexes. There is no doubt that a "realistic" solvent and crystal phase is a much more complex environment due to the strong interaction of every single Pd$(AcO)_2$/DMSO complex with neighboring molecules. Therefore one could expect a discrepancy between available crystal structures of Pd(II)/DMSO compounds and computationally evaluated relative stability of isolated S- and O-bond Pd$(AcO)_2$/DMSO within a simple two-DMSO model. Remarkably, our

larger model with two extra DMSO molecules agrees with available crystal structures of $Pd(AcO)_2$/DMSO.

Concluding, the $Pd(II)(AcO)_2(DMSO)_2$ model fails to predict the correct mode of DMSO bonding, but it provides a rather realistic description of metal-ligand geometry. In particular it delivers expected elongation/shortening of the O−S bond in DMSO with respect to O- or S-coordination, respectively (see Figure 2). The elongation of the Pd−O bond with respect to **b1** and **b2** and elongation of the Pd−S bond with respect to **b2** and **b3** are also expected. Underestimation of environmental effects is the evident downside of the model. Of important consideration, the energy difference between computationally identified $Pd(AcO)_2$/DMSO complexes is quite small when solvent effects are considered, and thus this discrepancy will not influence largely the overall reaction profile of reaction 1. It is quite difficult to achieve reliable convergence of complexes with "loosely bound" DMSO in the outer parts of the coordination sphere. The simplified two-DMSO model offers advantages in terms of computational convenience that are particularly important for a transition state search. The discrepancy between the O-bound and S-bound DMSO arrangement is quite small, and we proceed further within the simplified model, **b1**, of the catalyst, i.e., $Pd(II)(AcO)_2(DMSO\text{-}O)_2$.

$Pd(II)(AcO)_2(DMSO)_2$−Substrate Complexes in Polar Environment. Having studied the structure of palladium(II)/AcO_2 in DMSO solvent, we proceed further along the reaction pathway. Calculations indicate that the alcohol binds to the Pd(II)-catalyst **b1** or **b3** to form the very first activated complex (step B, Scheme 1) in the second coordination sphere with respect to Pd(II) (**c1** and **c2**, Figure 3). Similar catalyst resting state was characterized experimentally and with density functional theory for $Pd(OAc)_2$/Pyridine system (see ref. 2j, which remains the only example of in situ characterization of the catalyst under reaction conditions by spectroscopic rather than solely by kinetic methods). Also, an outer-sphere binding of the substrate was reported for a series of catalysts in ref. 3b,c, based on DFT calculations.

The electronic binding energy of the substrate is −7.4 kcal/mol. Two additional effects should be accounted for. First, an account for entropy decrease in the adduct **c1** is included in the Gibbs free energy correction of about 10 kcal/mol; binding becomes less favorable with this correction. Second, solvent effects should also be considered. Straightforward application of the continuum solvent model gives the following result: solvent stabilization, i.e., the absolute value of the energy that the molecule gains by interacting with solvent, is 40 kcal/mol for **b1**, 45 kcal/mol for **c1**, and 25 kcal/mol for the substrate. That equates to the total effect of +20 kcal/mol: the electronic energy of the reaction "**b1** + substrate → **c1**" is now about +13 kcal/mol taking into account the solvent effect within the continuum solvent model.

On the basis of the geometrical structure, it seems quite reasonable that **b1** and **c1** both have a similar solvent stabilization effect. However, the continuum solvent model overestimates the energy of the "**b1** + substrate" term. We have not accounted for a similar problem in our earlier studies mainly because we were concerned with nonpolar solvents, i.e., toluene.

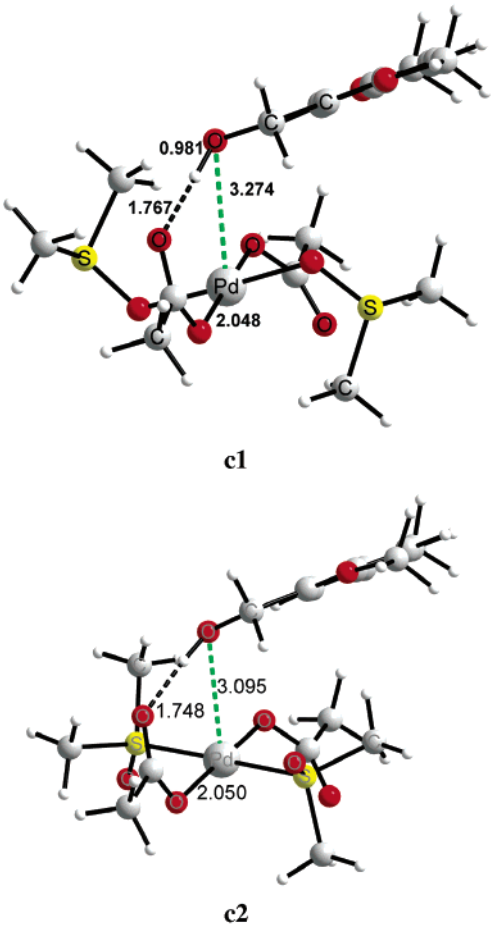

Figure 3. Optimized structure of $Pd(II)AcO_2(DMSO\text{-}O)_2$ and $Pd(II)AcO_2(DMSO\text{-}S)_2$ with (2,4-dimethoxyphenyl)-methanol coordinated in the second sphere. In the gas phase **c1** is more stable than **c2** by 4 kcal/mol. In the solvent the energy difference between **c1** and **c2** becomes almost negligible.

Geometry optimization of complexes larger than **c1** proved to be necessary to understand the solvent effects. To provide a realistic environment and yet to afford reliable geometry optimization, three DMSO molecules were added to the model. This extended model is described in detail in the Supporting Information. Evaluation of solvent effects within the extended model with additional DMSO points out that solvent effects are small when formation of adduct **c1** is considered in a realistic solvent environment. These effects are largely overestimated by straightforward application of continuum solvent model.

The Rate-Limiting Steps: The Deprotonation and the *β*-Hydride Elimination. The deprotonation of the alcohol (step C, Scheme 2) leads to the Pd-alkoxide complexes, **d1** and **d2**, which then undergo the *β*-hydride elimination step (step D, Scheme 2) to form the product and the Pd-hydride species. The reductive elimination of an equivalent of HX, i.e., AcOH, is necessary to form the Pd(0) resting state of the catalyst (E).

The *β*-hydride elimination has been proposed to be the rate-limiting step for the vast majority of the catalytic systems. This includes the systems derived from $Pd(OAc)_2L$ (where L = pyridine, PhenS,[7] I*i*Pr,[8]

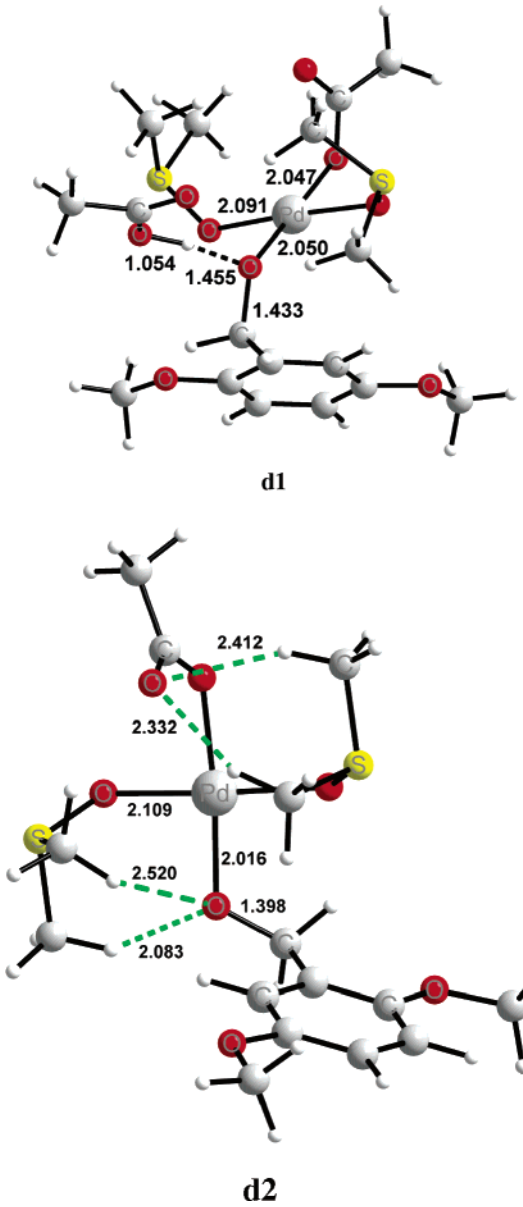

Figure 4. Optimized structure of Pd-alkoxide intermediate with and without AcOH: complexes **d1** and **d2**, respectively. All bond lengths and distances are in Å. Green dashed lines show weak intermolecular O−H bonds.

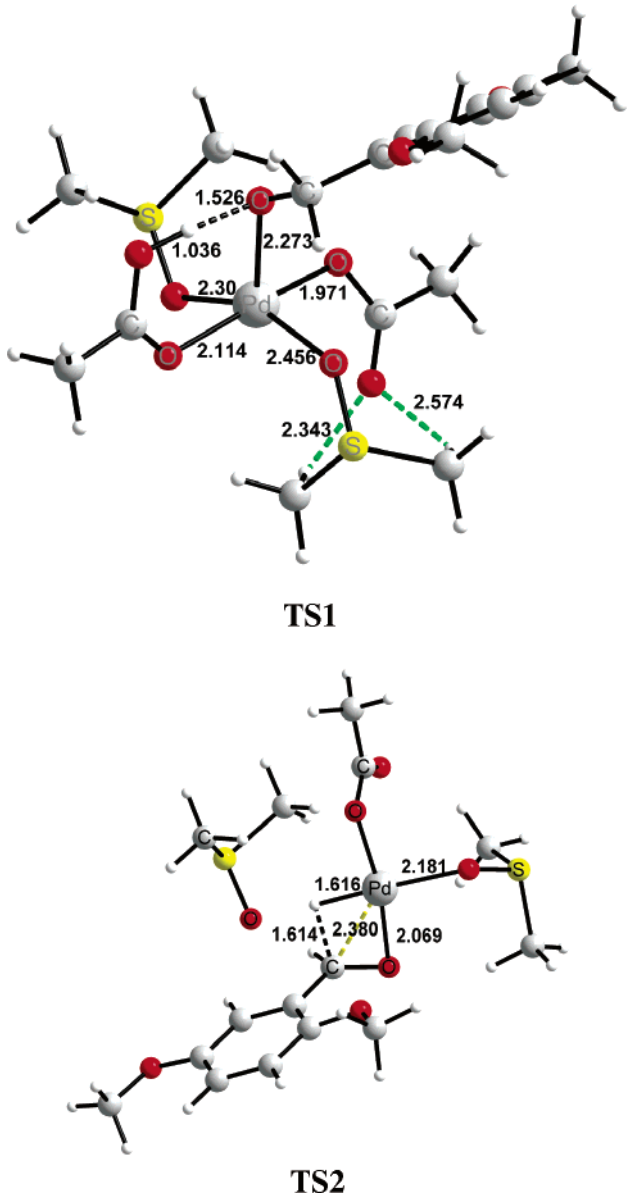

Figure 5. DFT-optimized transition states for the first deprotonation and the β-hydride elimination, TS1 and TS2, respectively.

Pd((−)-sparteine)Cl_2) with a strong base. The exception is Pd$(OAc)_2$/TEA,[2c] a Pd((−)-sparteine)Cl_2 catalyst under weak base conditions where the rate-limiting alcohol deprotonation is proposed and established both experimentally and theoretically. Interestingly enough, Larock's system, Pd$(AcO)_2$/DMSO, is currently also considered to have alcohol-related rate-limiting steps.[9]

To investigate alcohol-related transition states, the first deprotonation and the β-hydride elimination transition states were optimized (TS1 and TS2, Figure 5). Geometrical parameters of the first deprotonation and the β-hydride TS are similar to the previously reported data with respect to Pd$(AcO)_2$/pyridine and Pd$(AcO)_2$/TEA systems.

An alternative mechanism of the first deprotonation may be proposed. We have found that AcO^- interacts with additional DMSO molecules in the second coordination sphere. Thus it can be stabilized in the outer part of the coordination sphere without direct coordination to the metal ion (see Figure 6). This type of geometry is unfavorable without the consideration of a dielectric solvent environment. To provide insight into possible ligand arrangements, we have optimized the geometry of the substrate-catalyst adduct with AcO^- in the second coordination sphere supported by the intermolecular interaction with additional DMSO molecules (Figure 6). It is not possible to obtain such a "detached" AcO^- without additional solvent molecules: without additional DMSO complex **d1** with completely formed AcOH will be the result of the geometry optimization. Attempts were made to locate the corresponding TS of the alcohol deprotonation with the outer sphere AcO^-. So far we were not successful with this, mainly because the DMSO "cage" participates strongly in the rearrangement when

(7) PhenS = bathophenanthroline disulfonate, see ref 3e.
(8) IiPr = 1,3-bis(2,6-diisopropylphenyl)-2,3-dihydro-1*H*-imidazole; see ref 3h. Oxidation goes with added acid.

(9) Stahl, S. Private communication.

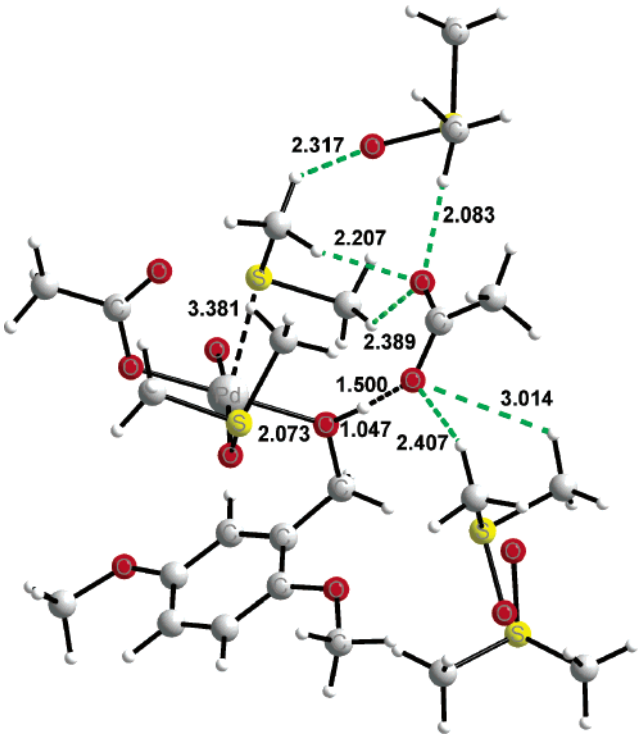

Figure 6. DFT/lacvp**-optimized geometry of substrate−catalyst adduct with AcO^- in the second coordination sphere supported by intermolecular interaction with additional DMSO molecules. Green dashed lines indicate intermolecular bonds. All distances are in Å.

AcOH is formed in the outer sphere. Thus, too many degrees of freedom are involved in the normal mode associated with such a hypothetical transition state.

Frequency analysis of the β-hydride TS reveals a relatively large imaginary frequency associated with the normal model of hydride transfer (the absolute value of the imaginary frequency is about 600 cm^{-1}). We have also identified the β-hydride TS with the S-bound DMSO. The electronic energy of this transition state is larger by 12 kcal/mol than that of TS with O-bound DMSO. However, we were not able to obtain information about environmental effects on the energy difference between the O- and S-mode TS with additional DMSO molecules. We have evaluated gas-phase-optimized TS geometries in the PCM. The energy difference was reduced to about 4 kcal/mol. Thus we expect that reaction may equally proceed via transition states with S- and O-bound DMSO.

The first deprotonation TS is dependent on the ligand environment and is characterized by a quite small imaginary vibrational frequency (the absolute value is about 60 cm^{-1}). We have found no "clean" TS when S-bound DMSO is considered. We have also found that the energy of the TS is dependent on the DMSO coordination in the outer sphere. We have attempted to locate the first deprotonation TS in the model with additional DMSO molecules. A precursor to TS was found, but we were not able to obtain the geometry with a single imaginary frequency. One could expect this, since many degrees of freedom prevents reliable identification of a low-energy vibrational mode.

The Gibbs activation energy of both transition states in solvent turns out to be in the expected range of 15 and 20 kcal/mol, respectively. The β-hydride TS is, in particular, somewhat higher than that for $Pd(AcO)_2$/TEA, but it is much smaller than that for $Pd(AcO)_2$/pyridine catalysts.

The optimized structure of the Pd-H complex immediately after the β-hydride elimination transition state (step D, Scheme 1) is reported in the Supporting Information.

From Palladium(0) to Palladium(II). The oxidation reaction proceeds further via a palladium(0)/DMSO intermediate, step E (see Scheme 1). The structure of the corresponding palladium(0) complexes is important for efficient reoxidation of the metal by molecular oxygen; it will be considered in detail further on. Formation of peroxo-palladium species has already been studied in detail.[10a,b]

Of principal consideration, the ground electronic state of molecular oxygen is known to be paramagnetic with two unpaired electrons. Due to the strong spin−orbit (SO) coupling, transition metal reactions are weakly spin forbidden, and a great deal of experimental data speaks in favor of efficient SO coupling involved. The oxygen-related palladium(0) reoxidation part of the catalytic cycle does not become rate limiting in the majority of the Pd-catalyzed reactions, including the presently studied system, ruling out spin−orbit-related bottlenecks with respect to the oxygen−metal pair. Furthermore, transition metal complexes are known to have a large number of near-degenerate electronic states. Near degenerate electronic states are well known to participate in metal−oxygen bond formation, and near-degeneracy further amplifies effective spin crossover.

The formation of the tight $Pd\text{-}O_2$ complex **e1** and **e2** is computed to be highly exothermic, $\Delta E = -46$ kcal/mol in the gas phase ($\Delta E = -44$ kcal/mol in solvent), and no barrier for that was found.[11] Triplet-to-singlet potential surface crossing permits formation of the η^2-peroxo complex (see Figure 7, complex **e2** with singlet electronic state) within tight meta-oxygen formations. Quite similar geometry and reaction energies for peroxo-$Pd(0)L_n$ complexes were reported previously by Stahl et al., where L is a nitrogen-based ligand. The crossover to the singlet surface is mediate by the spin−orbit coupling, which is generally efficient at transition metal centers.

Finally, the reaction of the peroxopalladium(II) species with 2 equiv of acid, AcOH, results in the step-by step restoration of original catalyst (steps G1−G3 in Figure 8). Hydrogen peroxide is formed within these final reaction steps. It turns out that these reaction steps are of no importance for the rate determination of the overall reaction and are very similar to those previously reported for Pd-systems with pyridine or TEA ligands (see ref 3b), and therefore the corresponding complexes are discussed in the Supporting Information only.

(10) (a) Pd-mediated activation of molecular oxygen in a nonpolar solvent medium has been studied: Keith, J. M.; Nielsen, R. J.; Oxgaard, J.; Goddard, W. A., III. *J. Am. Chem. Soc.* **2005** ASAP article. (b) Stahl et al. has shown that in the case of palladium(0) complexes with nitrogen-based ligands spin crossover dynamics do not influence the overall oxygenation kinetics; see: Landis, C. R.; Morales, C. M.; Stahl, S. S. *J. Am. Chem. Soc.* **2004**, *126*, 16302−16303.

(11) No barier was found in previous theoretical studies. Surprisingly, the same values of O−O and Pd−O distances have been found in our and Stahl's η^2-peroxo complex, 1.40 and 2.02 Å, respectively. The distance between Pd and oxygen from DMSO is 2.16 Å, almost the same as in complex $Pd^0(DMSO\text{-}O)_2$ (2.15 Å).

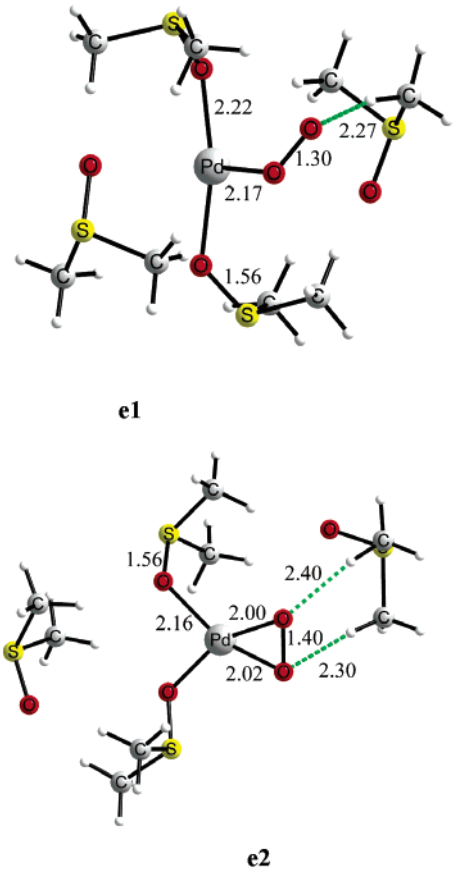

Figure 7. Gas-phase-optimized structure of the Pd^0-$(DMSO\text{-}O)_2$ complex with molecular oxygen. The electronic states of **e1** and **e2** are triplet and singlet, respectively. All distances are in Å.

Pd(0)/DMSO Intermediates: Hard (O) versus Soft (S) Ligand Donor Atoms. Insight into reaction 1 would be incomplete without consideration of palladium(0) complexes in DMSO. The ambidentate character of DMSO plays an important role in the formation of Pd(0)/DMSO complexes. To begin probing this subject, we have optimized $Pd(0)(DMSO)_2$ complexes with S- and O-bound DMSO. The S-bound coordination mode of DMSO was preferable, with the electronic energy lower by almost 10 kcal/mol than that of the O-bound analogue. Continuum solvent effects reduced this energy difference by only 2 kcal/mol.

Gas-phase and solvent geometry optimization of larger complexes revealed that the two most stable complexes of Pd(0)/DMSO, see Figure 9, have up to four S-bound DMSO ligands in the first coordination sphere, $Pd^0(DMSO\text{-}S)_4$. The tetrahedral geometry in which palladium(0) is in the center of the tetrahedron and sulfur atoms are at each vertex[12] is shown in structure **f1**. This type of geometry is not surprising, since palladium(0) has the d^{10} configuration with preferable tetrahedral ligand arrangement.[13]

Complex **f2** has a slightly distorted arrangement of the ligand with two slightly shortened and two slightly elongated Pd−S bonds. We have also identified several

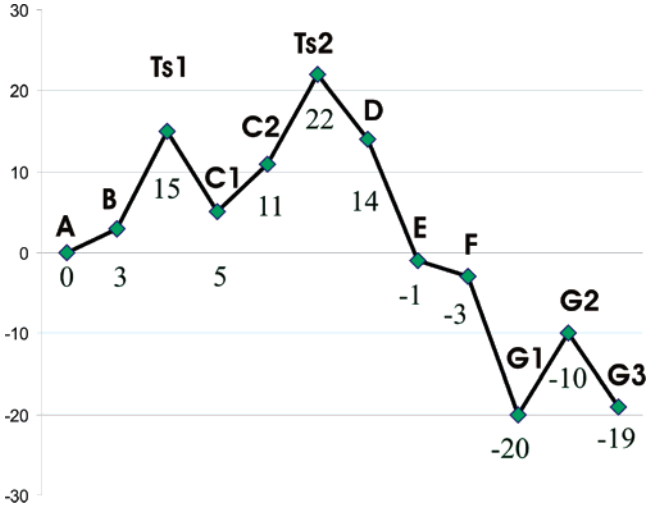

Figure 8. Computed reaction profile (Gibbs free energy) according to the reaction mechanism for Scheme 2. Labels Ts1 and Ts2 indicate the first deprotonation and the β-hydride elimination transition states, respectively. All reaction steps follow the uppercase assignment used in Scheme 1. Assignment of these reaction steps to the lowercase letter labels of computed important structures is the following: step A involves complex **a**; step B involves complex **c1** or **c2**; steps C1 and C2 involve complexes **d1** and **d2**, respectively; step D involves Pd−H complex (see Figure S9 in the Supporting Information); step E involves Pd(0)/DMSO complexes **g** or similar; step F involves complex **e2**. The last three labels, G1−G3, refer to $PdO_2/(AcOH)_x$ complexes (see Figure S7 in the Supporting Information). All energies are in kcal/mol with solvent effects. The solvent was modeled using the hybrid method, which is polarized medium (PCM) with additional DMSO molecules in the second coordination sphere of the Pd-complexes and reactants, i.e., molecular oxygen, substrate, AcOH.

complexes with mixed S- and O-bonding (in our opinion **f3** is the most interesting one). Those complexes, including **f3**, are higher in energy than **f1** and **f2**. Continuum solvent effects evidently favor complexes with S-bound DMSO. One may argue that S-bound DMSO leaves the O atom in the outer part of the coordination sphere, which is perfectly suited for interaction with additional DMSO molecules. O-bound DMSO lacks this additional coordination capability. This was checked by geometry optimization of large complexes of palladium(0) in DMSO. Interestingly, coordination geometry of just three DMSO-S has been found in a large cluster with two palladium(0) atoms (Figure 10). Because of the size of the complex, we had to employ a smaller basis set for this geometry optimization.

DMSO has the remarkable ability to coordinate palladium(0). We have found that a large variety of palladium(0)-DMSO-palladium(0) structures could be optimized. One of those structures is presented in Figure 11. We have also found that palladium(0) dimers could be bridged by several DMSO molecules in the outer coordination spheres of both metals without direct coordination to the metal in either the S- or O-bound mode.

(12) Geometry optimization of the Pd(0) with up to eight DMSO ligands was carried out in the gas phase and solvent (PCM). The first coordination sphere of Pd(0) could hold only four sulfur-bonded DMSO; additional ligands were weakly coordinated in the second coordination sphere.

(13) Within the d^{10} electron configuration of Pd(0) every d orbital is doubly occupied. Symmetric electron distribution means that there are no ligand field effects and the ligand positions are sterically determined.

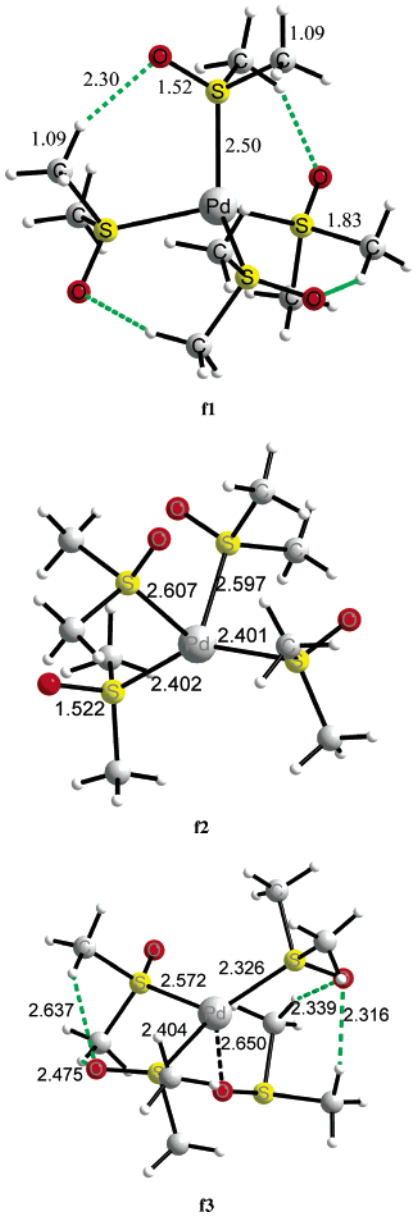

Figure 9. Optimized structure of sulfur-bonded Pd(0)-(DMSO-S)$_4$ complexes with sulfur-bonded DMSO, DMSO-S. Dashed green lines indicate weak H-bonds. All distances are in Å; symmetry constraints were not employed. The energy of **f2** is only 2.5 kcal/mol lower than that of **f1**. Complex **f1** has almost perfect tetrahedral ligand arrangement. The energy of **f3** is about 3 kcal/mol higher than that of **f1**.

Hydrogen bonds appear to be important for the stability of isolated Pd/DMSO complexes. The same seems to be true for large DMSO complexes. In particular, the Pd(0)(DMSO-S)$_4$ structure of the first coordination sphere is stabilized by four hydrogen bonds between oxygen and hydrogen atoms. The distance between oxygen and hydrogen atoms, 2.30 Å, is shorter than the sum of the van der Waals radii, 2.72 Å, while the C−H−O angle is 150°. The H-bond (X-H···Y) is formed due to the transfer of the electron density (ED) from the lone electron pairs of the proton acceptor Y to the σ^*-antibonding orbital of the X-H proton donor.[14] DFT calculations revealed typical elongation of the C−H bond, 0.001 Å, and significant increase of the electron density in the σ^*-antibonding CH orbital, 0.01189*e*.[15]

Binding of DMSO to palladium(0) with the oxygen atom dramatically changes the geometry of the first coordination sphere of the Pd(0)/DMSO complex (see Figure 12). DFT geometry optimization of large systems, i.e., Pd(0)/(DMSO)$_{12}$, suggests firmly that not more than two DMSO molecules could be oxygen-bound to the metal in the first coordination sphere, while additional ligands could be accommodated in the very symmetrical second coordination sphere only. We denote this type of coordination presented in Figure 12 as Pd(0)(DMSO-O)$_2$[DMSO]$_2$, with two oxygen-bound DMSO in the first coordination sphere and two additional DMSO molecules in the outer sphere. The metal−oxygen distance is 2.15 Å in complex **g**, while the sulfur−oxygen distance is just 0.04 Å longer than in the free DMSO. The experimental bond elongation in DMSO is 0.036 Å. The rearrangement of the first coordination sphere from **f1** to **g** requires energy: the electronic energy of complex **g** is higher than that of complex **f1** by 10 to 12 kcal/mol.

Conclusions

Computational studies provide insight into the reaction mechanism of Pd-catalyzed alcohol oxidation and into coordination of the DMSO ligand to palladium(0) and palladium(II). The reaction mechanism consists of three distinctively different parts, which are all characterized in the present study. The first part directly relates to the catalyst−substrate interaction and proceeds via two transition states: the first deprotonation and the β-hydride elimination transition states. Modern computational tools make it relatively easy and straightforward to optimize geometry of these transition states and evaluate accurate electronic energies. Reported data appear to be in agreement with previously published findings.

The second part of the reaction is more delicate and less straightforward to model. Experimental data indicate that the reaction proceeds via Pd(0)(DMSO)$_x$ complexes. Therefore we have started with finding out the coordination geometry of Pd(0)(DMSO)$_x$, with O- and S-bound solvent. We have seen that environmental effects are important for stability and geometry of palladium/DMSO complexes. This relates equally to palladium(0) and palladium(II). To check if soft DMSO-S cages are stable in the complex solvent environment, we have considered large palladium(0) complexes with two metal centers and a large quantity of explicitly treated DMSO molecules. Stable Pd(0)(DMSO-S)$_n$ ($n = 3, 4$) complexes were identified computationally in DMSO environment. One may conclude that Pd(0)-(DMSO-S)$_3$ and Pd(0)(DMSO-S)$_4$ complexes with additional DMSO molecules in the outer coordination sphere are stable enough against small rearrangements of the inner coordination sphere of palladium.

The third and final part of the oxidation reaction involves interaction of O_2 with palladium(0)/DMSO

(14) This effect is well known in physical organic chemistry and is called hyperconjugation.

(15) Hydrogen bonding is characterized by the elongation of the X−H bond, a decrease of its stretch frequency, and an increase of intensity of the respective spectral band. An increase of ED in the σ^* orbital is accompanied by weakening of the corresponding bond and its elongation and a concomitant lowering of the X−H stretch frequency.

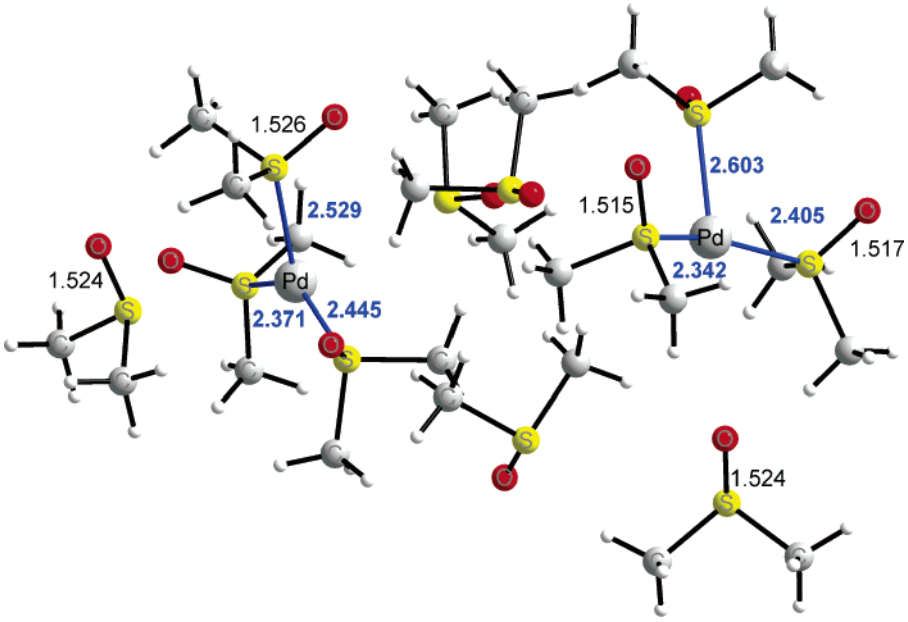

Figure 10. B3LYP/lacvp-optimized molecular cluster with two palladium(0) atoms and DMSO molecules. Blue lines mark S-palladim(0) bonds of the DMSO-S ligand. Corresponding bond length labels are in blue. S−O bond distance in "free" DMSO is in black. Smaller basis set results in slightly longer Pd-S bond length, as compared to leap** base set results.

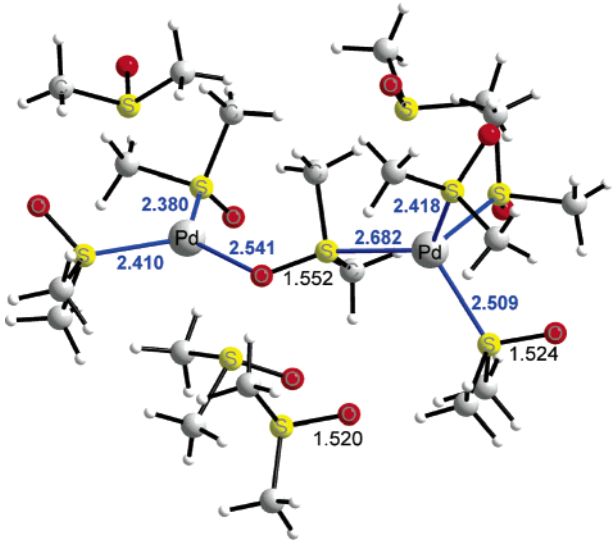

Figure 11. B3LYP/lacvp-optimized molecular cluster with two palladium(0) atoms bridged by a DMSO molecule in the cluster of DMSO molecules. Blue lines mark DMSO−palladim(0) bonds. Corresponding bond length labels are in blue. S−O bond distance in "free" DMSO is in black.

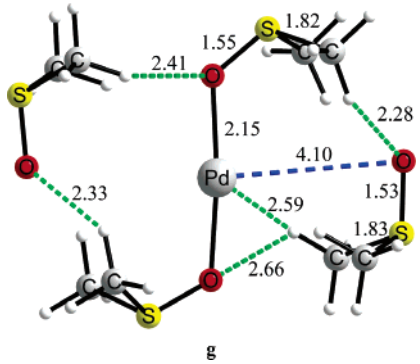

Figure 12. Optimized structure of the oxygen-bonded Pd-(0)(DMSO-O)$_2$[DMSO]$_2$ complex with two oxygen-bonded ligands in the first coordination sphere. All distances are in Å. Palladium(0) is accessible from the directions above and below the coordination plane defined by palladium, oxygen, and sulfur atoms. Dashed green lines indicate weak H-bonds.

complexes. The soft ligand cage in the Pd(0)(DMSO-S)$_4$ complex is able to prevent O_2 from reaching the metal directly. The most probable coordination mode of molecular oxygen is to be bound in the second coordination sphere with respect to Pd(0)(DMSO-S)$_4$. This was computationally verified by geometry optimization of Pd(0)(DMSO-S)$_4$[O_2] complexes. Of important consideration, Pd(0)(DMSO-S)$_4$[O_2] could be an important element of the considered reaction pathway. Indeed, considerable separation between palladium(0) and O_2 in Pd(0)(DMSO-S)$_4$[O_2] could in principle provide rate limiting and lower the efficiency of spin crossover. Thus, the oxidation reaction on the metal would be rate limited in this scenario. If experimental data would suggest that O_2-related steps are rate limiting, Pd(0)-(DMSO-S)$_4$[O_2] complexes would be the answer as to why that might be.

However, both the importance of Pd(0)(DMSO-S)$_4$[O_2] complexes to the oxidation reaction and the stability of such complexes are undermined by the influence of the solvent environment. Computational results suggest that Pd(0)(DMSO-S)$_3$ complexes are able to equilibrate easily with Pd(0)(DMSO-S)$_2$[DMSO-O] complexes in the presence of complex ligand environment. Those complexes have quite flexible and open ligand arrangement; there is also enough coordination volume to accommodate Pd(0)−O_2 bonding. Therefore it is quite reasonable to suggest that Pd(0)O_2 complexes will be readily formed in DMSO. This reasoning appears to be coherent with a recent experimental finding[9] concerning rate-limiting steps in reaction 1.

Overall, our computational studies are performed within a well-tested model and the acquired data agree very well with available kinetic experimental data for reaction 1 and for the first time provide elucidation of

the nature of the rate-limiting step. We point out that S-bound or O-bound DMSO is the preferable coordination mode of palladium(II) depending on the ligand environment, while palladium(0) prefers mainly S-bound DMSO.

Technical Details

The following computational methodology was applied. First, geometry optimizations of all intermediate complexes and transition states were carried out using the B3LYP functional[16] with the lacvp**/6-31G(d,p) basis set.[17,18] All degrees of freedom were optimized, and only positive vibrational frequencies were obtained at all optimized geometries. Transition states obtained were characterized by the presence of exactly one imaginary vibrational frequency along the appropriate normal mode. In the second step, B3LYP energies were evaluated for the optimized geometry using a much larger triple-ζ basis, lacv3p**+/6-311+G(d,p), with additional diffuse and polarization functions. These energies together with the solvent and the thermochemical corrections were used to calculate the reported reaction profile. Large "supercomplexes" with two palladium atoms were not checked by frequency analysis, and the geometry was optimized with the lacvp basis set.

All computations were performed with the Jaguar v4.0 and v6.0 suite of ab initio quantum chemistry programs.[19] Solvent (DMSO) was represented with the following parameters: $\epsilon = 49.0$ and probe radius $r_p = 2.415$ Å. The solvent was modeled using the polarized medium (PCM) with additional DMSO molecules in the second coordination sphere of the complexes studied. Solvent effects related to "small molecules", i.e., O_2 and the substrate, were double checked by explicit treatment of the coordination sphere in an extended DMSO supercluster of 36 solvent molecules at the same level of accuracy as the reported geometry optimizations. A similar type of superclusters was used for an estimation of solvent effects.

All gas-phase-optimized structures of complexes studied were found to be accurate enough and were used to estimate solvent effects on the reaction energy within the self-consistent reaction field model as implemented in the Jaguar computational package.

Finally, complete thermochemical analysis and additional transition state searches were performed with the Gaussian 98[20] computational package within the restricted DFT/B3LYP level of theory and with the LanL2DZ[21] basis set. All the structures of the intermediate complexes and transition states were reoptimized with this smaller basis set prior to the computation of harmonic vibrational frequencies.

Acknowledgment. The authors wish to thank Carl Tryggers Stiftelse for the PostDoc fellowship (W.Z.). Computer time at Poznan and Wrocław Supercomputer and Networking Centers and SNAC allocation of computer time at NSC, Linköping, are greatly acknowledged. We thank Professor Matthew S. Sigman for fruitful discussion.

Supporting Information Available: XYZ-coordinates, energies, and structural parameters of optimized complexes, as well additional supporting data including evaluation of crystal structures. This material is available free of charge via the Internet at http://pubs.acs.org.

OM0506217

(16) (a) Becke, A. D.; *J. Chem. Phys*. **1993**, 98, 5648. (b) Lee, C.; Yang, W.; Parr, R. G. *Phys. Rev. B* **1988**, *37*, 785−789.

(17) Hay, P. J.; Wadt, W. R. *J. Chem. Phys*. **1985**, *82*, 299−310.

(18) (a) Hehre, W. J.; Ditchfield, R.; Pople, J. A. *J. Chem. Phys*. **1972**, *56*, 2257−2261. (b) Francl, M. M.; Pietro, W. J.; Hehre, W. J.; Binkley, J. S.; Gordon, M. S.; Defrees, D. J.; Pople, J. A. *J. Chem. Phys*. **1982**, *77*, 3654−3665. (c) Hariharan, P. C.; Pople, J. A. *Theor. Chim. Acta* **1973**, *28*, 213−222.

(19) *Jaguar 4.0*; Schrödinger, Inc.: Portland, OR, 1991−2000.

(20) Frisch, M. J.; Trucks, G. W.; Schlegel, H. B.; Scuseria, G. E.; Robb, M. A.; Cheeseman, J. R.; Zakrzewski, V. G.; Montgomery, J. A., Jr.; Stratmann, R. E.; Burant, J. C.; Dapprich, S.; Millam, J. M.; Daniels, A. D.; Kudin, K. N.; Strain, M. C.; Farkas, O.; Tomasi, J.; Barone, V.; Cossi, M.; Cammi, R.; Mennucci, B.; Pomelli, C.; Adamo, C.; Clifford, S.; Ochterski, J.; Petersson, G. A.; Ayala, P. Y.; Cui, Q.; Morokuma, K.; Malick, D. K.; Rabuck, A. D.; Raghavachari, K.; Foresman, J. B.; Cioslowski, J.; Ortiz, J. V.; Baboul, A. G.; Stefanov, B. B.; Liu, G.; Liashenko, G.; Piskorz, P.; Komaromi, I.; Gomperts, R.; Martin, R. L.; Fox, D. J.; Keith, T.; Al-Laham, M. A.; Peng, C. Y.; Nanayakkara, A.; Challacombe, M.; Gill, P. M. W.; Johnson, B.; Chen, W.; Wong, M. W.; L.Andres, J.; Gonzalez, C.; Head-Gordon, M.; Replogle, E. S.; and Pople, J. A.; *Gaussian 98*, *Revision A.9*; Gaussian, Inc.: Pittsburgh, PA, 1998.

(21) The use of the effective potential LanL2DZ basis set for thermochemical analysis, namely, for acquiring thermodynamic functions and Gibbs free energy, has regularly been found to result in a level of accuracy comparable to that of superior basis sets to a small fraction of computational costs.